Elastic-bracing and its potential effect on seismic waveforms in reservoir injection zones

Kris Innanen, Don Lawton and Malcolm Bertram

ABSTRACT

Comparisons of seismic waveforms propagating through geological formations, before and during injection of microbubble water and/or CO_2, are suggestive of dynamic effects that cannot easily be explained with normal linear elastic theory. A characteristic change in the coda, a strong loss of low frequency energy, and a moderate increase of high frequency energy have been noted. Rather than appealing to linear elastic wave theory coupled with an unrealistic level of new heterogeneity, we point out that homogeneous elastically-braced media produce all three of these features in a propagating waveform as first order effects. A modified Klein-Gordon equation is used to replicate behaviour in a published microbubble injection experiment, and similar features are sought in a raw VSP data set acquired before and during injection of CO_2 at the CaMI-FRS in November 2018. Early indications are that the two spectral changes explainable via Klein-Gordon waves can indeed be seen in the VSP data, but issues such as source coupling repeatability must yet be eliminated as factors. If the new bracing parameter η introduced to reproduce these data features macroscopically quantifies transient fluid properties, determination and mapping of this parameter would provide a new mode of seismic characterization of injection.

INTRODUCTION

In two independent time lapse seismic experiments (one carried out by CREWES and one not), changes have been observed in the seismic waveforms transiting a fluid injection zone which are difficult to explain in the context of standard linear acoustic/elastic wave theory. The three unusual features of the waveforms propagating through the fluid in comparison to the baseline waveforms are (*i*) a strong suppression of low frequencies, (*ii*) a weak increase of high frequencies, and (*iii*) a change in the time-domain coda. The injection fluids (CO_2 in one case, microbubble water in the other) have in common the presence of a suspension of bubbles whose mechanical effect on the geological volume may be quite complex. In this paper no mechanical explanation is put forward, but a macroscopic interpretation, namely that the injection fluids are causing the seismic disturbance to act as if it is occurring in an *elastically-braced* medium, is set out. An elastically-braced medium is one in which a disturbance is resisted by a second restoring force, in addition to the standard Hooke's law, proportional to the displacement. A wave propagating in a homogeneous elastically-braced medium undergoes three main additional changes which match (*i*)-(*iii*) above. Waves on an elastically-braced string are described by the Klein-Gordon equation; waves in an elastically-braced geological volume require a change to be made to the elastodynamic equations causing them to take on an "elastic Klein-Gordon" form. In this context seismic disturbances in a 3D elastically-braced medium can be simulated, and many of the bulk features of the two injection experiments reproduced.

EXPERIMENTAL MOTIVATION

The geophysics literature contains many examples of time-lapse (or 4D) seismic experiments and analyses, but there are very few instances in which a careful comparison of raw waveforms within baseline and monitoring surveys are included. Instead, generally a 4D signal is interpreted following a significant processing regimen and data reduction effort. The tendency to "process away" unexpected data features is necessary in time-lapse studies, as irrelevant variations are always present in practice and these interfere with the interpretation. However, one unfortunate outcome of this is that the question:

> *How common is it for complex seismic waveform changes to be produced by the introduction of fluids/gases/mixed phases into a reservoir?*

...is difficult to answer with a literature search. Anecdotally and otherwise, changes of this kind do seem to happen. In this paper, two instances will be referred to. One instance is taken from a time lapse experiment carried out by JOGMEC in 2016; the other is a CREWES-CaMI experiment carried out in October-November of this year. Both contain evidence of persistent, difficult-to-explain temporal and/or spectral characteristics which point to unusual mechanical phenomena.

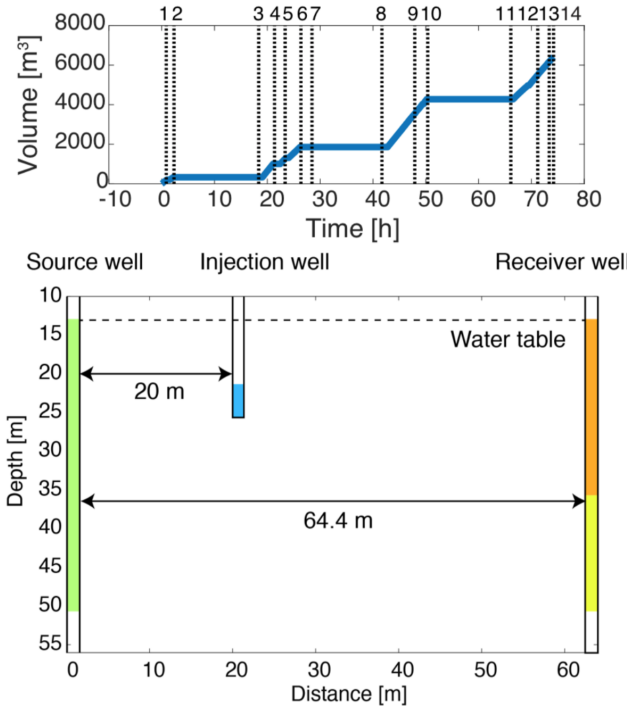

FIG. 1. From Kamei et al. (2017); used by permission. Geometry and schedule of a JOGMEC microbubble water injection monitoring experiment. Top panel: fluid injection schedule over the 80hr experiment; periods of rapid injection and quiescent periods are present. Bottom panel: crosswell geometry (source and receiver boreholes) and injection zone.

The JOGMEC microbubble crosswell experiment

Kamei et al. (2017) reported on a JOGMEC study designed to validate full waveform

inversion as a tool for monitoring of near-surface microbubble water injection. In Figure 1 (top panel) the injection schedule highlights periods of injection interspersed with quiescent periods over a full injection interval of 80hrs. In the bottom panel the geometry of the injection and monitoring is illustrated (a roughly 50×50m volume of sands and silts). The source and receiver wells bracket the injection zone.

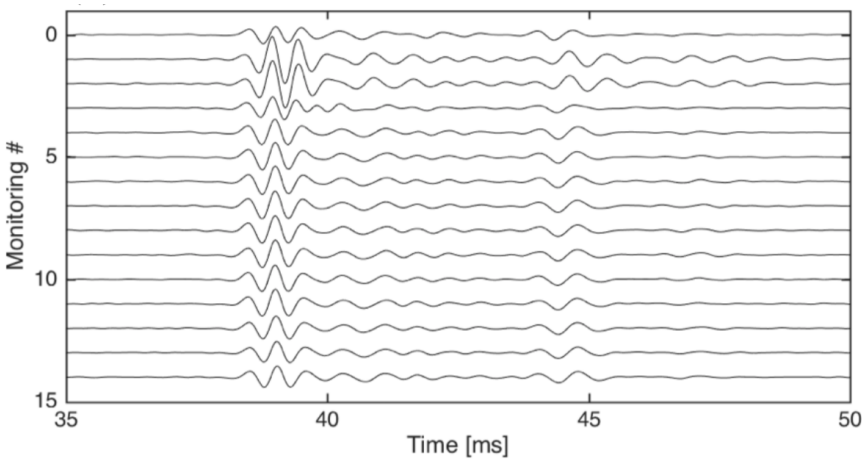

FIG. 2. From Kamei et al. (2017); used by permission. Traces from a single cross-well source-receiver pair at 16 monitoring points during the 80hr experiment. Top and bottom traces exhibit almost perfect repeatability. During the first 5 monitoring shots, significant waveform changes are induced by the presence fo the microbubble water.

In the same paper the waveforms at various stages before, during and after the injection are plotted. In Figure 2 an example is extracted from the paper. These traces are all from the same source-receiver pair, with the vertical axis representing monitoring stage number (i.e., the horizontal positions in the top panel of Figure 1). The repeatability of the cross-well acquisition was tested carefully, and thus the waveform differences plotted here represent the effects of the microbubble fluid on the seismic energy transiting the injection zone. The top and bottom traces illustrate the baseline state of the medium, which is returned to by the end of the experiment; the traces within the first 5 monitoring points exhibit the behaviour of current interest.

Figure 3 was shared with the authors by JOGMEC and is used here by permission. Traces from hours 1 and 74 are replotted in Figures 3a-b (top); more importantly, the spectra of these same traces are plotted below. There are 3-4 peculiar features of the traces at 1hr versus those at 74hrs: (1) the introduction of a coda; (2) the suppression of low frequencies; (3) the slight boosting of high frequencies; and (4) a notch. These features were all pointed out to CREWES researchers by Mouri, Kato and Kurosawa in 2016 as oddities requiring explanation.

The CaMI-FRS CO_2 VSP experiment

The Containment and Monitoring Institute (CaMI) maintains and operates a field research station (FRS) in Newell County AB; seismic experimentation at this site is the focus of CREWES field operations this year. The purpose of the site is to inject CO_2 into formations at 300m and 600m depths within a geologically and geophysically well-characterized

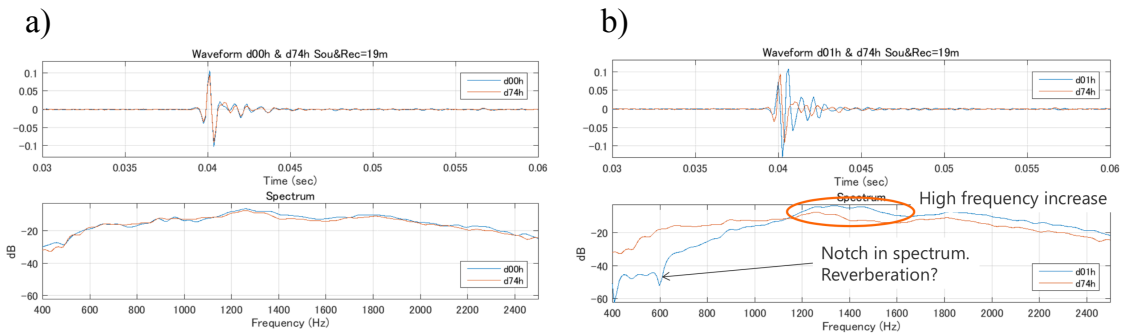

FIG. 3. Adapted from JOGMEC data QC slides (used by permission). Time domain (upper panels) and frequency domain (lower panels) plots of the response of a single crosswell source-receiver pair. (a) Traces at hours 0 and 74, i.e., the beginning and end of the experiment; (b) traces at hours 1 and 74. The spectral response appears to be entirely due to the introduction of the microbubble water.

volume, and test a range of geophysical, geological, and geochemical monitoring techniques (Lawton et al., 2015). Amongst the geophysical infrastructure in place at the CaMI-FRS are a permanent array of 3C geophones within the geophysics well.

In the Fall of 2018, injection of CO_2 was brought online, and simultaneously a range of innovative seismic data acquisition initiatives were begun, including: design and deployment of a prototype multicomponent fibre-optic seismic sensor (Innanen et al., 2018); a 3D DAS+3C walkaway walkaround vertical seismic profile dataset to support full waveform inversion and DAS research; deployment of a permanent source for quasi-continuous seismic monitoring (Spackman and Lawton, 2018); deployment and data from a land streamer (Lawton et al., 2018).

On this backdrop, a simple experiment was carried out before and during a several-hour injection interval. The University of Calgary Envirovibe Vibroseis source was positioned to direct seismic energy past the injection well and into the borehole phones. A baseline shot was recorded, and after several hours of injection a monitoring shot was likewise recorded. The vertical component traces are plotted in Figure 4.

Visually in the time domain there is little evidence of variation (see for example trace 2 in Figure 5a); repeatability appears to be qualitatively very good.

In the frequency domain, however, a persistent and significant variation is noted across all traces. During injection the low frequency components of the spectrum are strongly suppressed and the higher frequency components are mildly boosted. See Figure 5b.

Summary

Both of these examples are from field studies, and so a range of differences between baseline and monitoring surveys must be assumed to be present. Source coupling issues, for instance, and source positioning accuracy must be viewed as possible contributors to the observed signal. Nonetheless, these changes to the waveform when it propagates through complex fluids are difficult to ignore, and are difficult to explain using standard elastic and/or acoustic wave theory without invoking unrealistic degrees of altered heterogeneity.

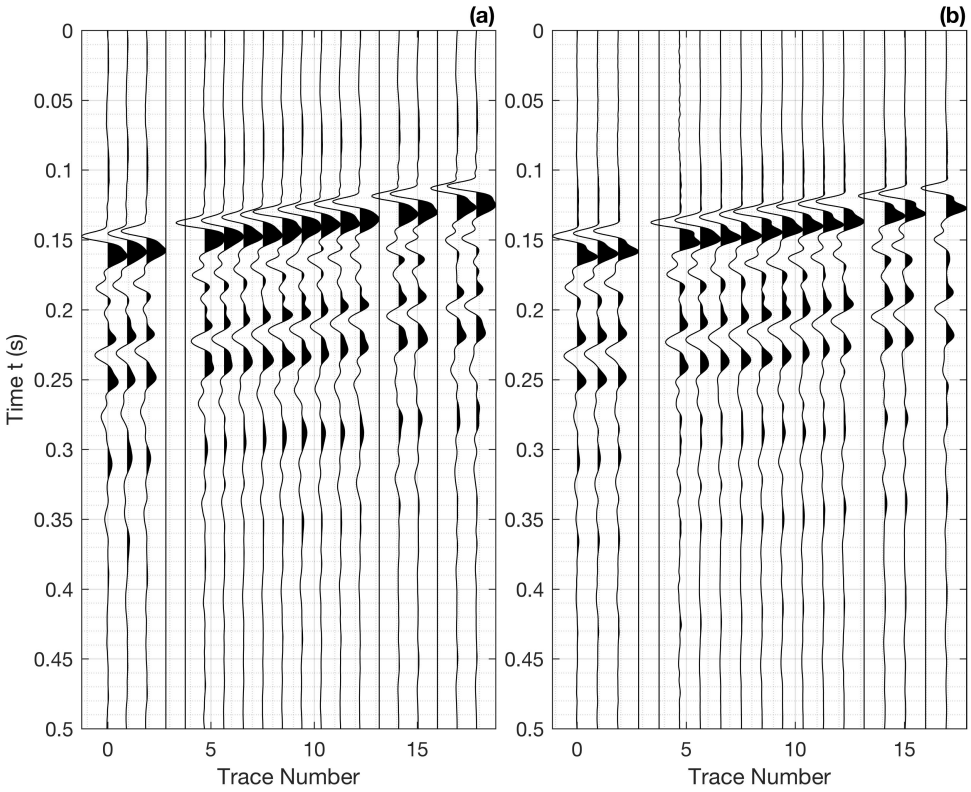

FIG. 4. Shot records into downhole permanent array (vertical component), with dead phones zeroed. (a) Prior to injection; (b) After 3-4 hrs of injection. Geophone counter increases in decreasing depth order.

ELASTIC BRACING AND THE KLEIN-GORDON EQUATION

In the mid 1920s, a rapid sequence of theoretical advances were made leading to modern quantum mechanics. One of the original formulations of the quantum description of electrons and their behaviour took the form of an equation, discovered by Schrödinger, which was strongly akin to a wave equation. The main failing of the equation (amongst its many successes) was that it was not relativistically invariant, meaning that it was inconsistent with special relativity and therefore could not be expected to properly describe particles moving near c. Schrödinger was aware of this issue—in fact, an earlier version of his equation for the electron he had written down *was* relativistically invariant, but he was forced to abandon it because it produced incorrect predictions*. He was later (and perhaps unfairly) judged to have been too timid in not publishing this equation, because it turned out to be very important in the description of other quantum systems. O. Klein and W. Gordon were less concerned about its issues with respect to experiment, and were eventually credited with its discovery.

*The combination of relativity and quantum mechanical equations as Schrödinger attempted it was doomed, because it was being attempted without including spin.

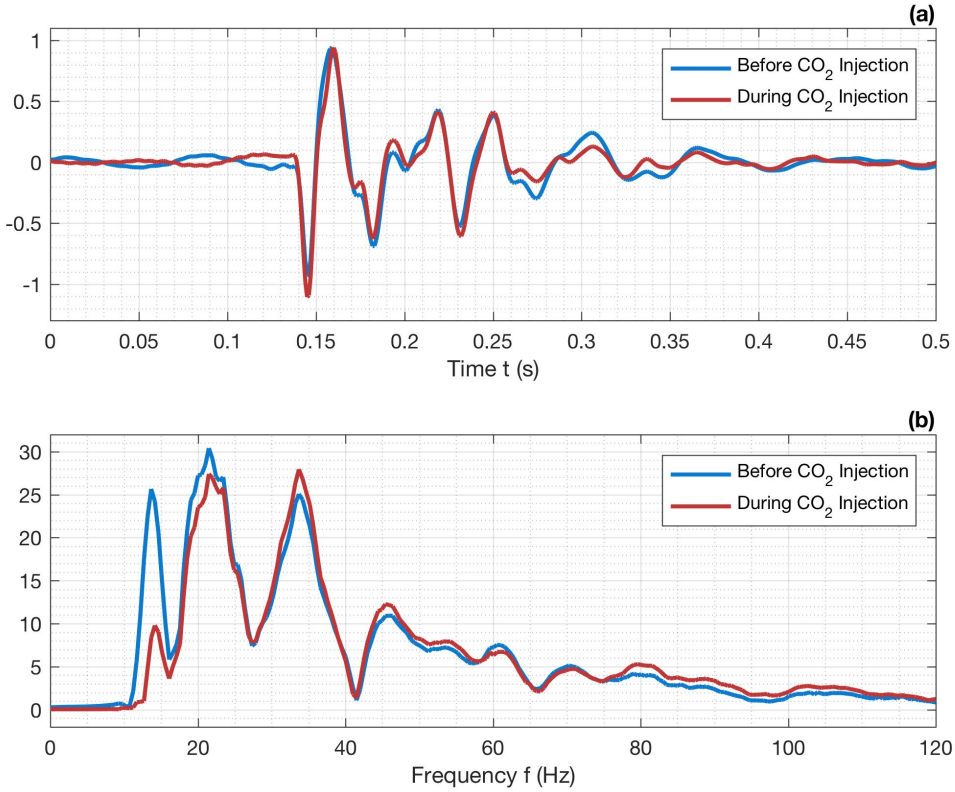

FIG. 5. Detail and spectra for geophone position 2 (second from bottom). (a) Geophone 2 response during baseline and monitoring shots, time domain; (b) geophone 2 response during baseline and monitoring shots, frequency domain (i.e., amplitude spectra).

Elastic bracing

Morse and Feshbach (1953) discuss the Klein-Gordon (KG) equation not in terms of its quantum interpretation, but in terms of its classical interpretation involving waves on a string. M & F provide the standard derivation of the wave equation involving a vertical displacements of a string fixed laterally under tension. They point out that, were the string to be embedded in (e.g., glued to) a sheet of rubber, such that in addition to the restoring force provided by the tension in the string, an additional Hookean resistance to displacement were added, the result is the KG equation. See Figure 6.

Waves on a braced string and the Klein-Gordon equation

The M & F discussion begins with the derivation of the behaviour vertical displacements u of the free string under tension:

$$\partial_{tt}u(x,t) - c^2\partial_{xx}u(x,t) = 0, \tag{1}$$

i.e., the standard wave equation, and then extends this to describe displacements of the braced string:

$$\partial_{tt}u(x,t) - c^2\partial_{xx}u(x,t) + 2\eta\, u(x,t) = 0, \tag{2}$$

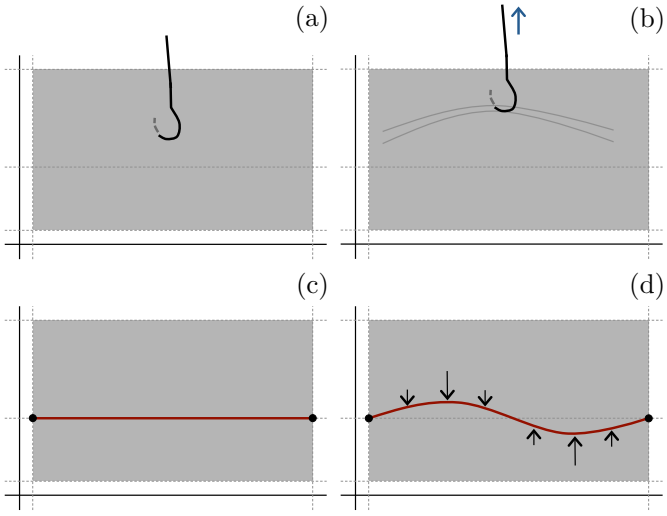

FIG. 6. The physical backdrop for the classical interpretation of the Klein-Gordon equation. (a)-(b) A coordinate system is set up referring to a plane with lateral and vertical directions; in this plane a sheet of rubber is stretched. (c)-(d) On this sheet of rubber a taut string is glued, such that at any point along the string disturbances in the vertical direction are opposed by both the string tension and the elastic sheet. The outcome of this configuration is an equation describing displacements of the string mathematically consistent with the quantum Klein-Gordon equation.

which is the 1D KG equation. Notice that to characterize the wave motion of an elastically braced string, a single additional parameter η (not the terminology used by M & F), the elastic constant of the rubber sheet, is introduced in addition to the wave velocity c.

Numerical features of 1D solutions

Solutions of the KG equation in a homogeneous medium naturally reproduce the features noted in both of the fluid injection wave problems, suggesting that an equation of this type might be active in regions with complex combinations of liquid and gas. We posit no mechanical model in this paper; evidence is purely circumstantial. To observe these aspects of braced wave propagation, we adapt the 1D finite difference updating formula for the discrete field u_i^n at position i and time n, obtaining for the $n+1$th time point:

$$u_i^{n+1} = 2\left[1 - \left(\frac{c\Delta t}{\Delta x}\right)^2 - \eta\right] u_i^n + \left(\frac{c\Delta t}{\Delta x}\right)^2 \left[u_{i-1}^n + u_{i+1}^n\right] - u_i^{n-1}. \tag{3}$$

The presence of the coefficient η is what sets this equation apart; setting $\eta = 0$ causes the equation to lapse to the standard form of the wave equation.

In Figure 7, snapshots of a Gaussian pulse propagating in the positive x direction are plotted such that we may observe the variation in its propagation when controlled by the classical wave equation (in red) versus the KG equation (in black). The dispersion and change in the low frequency components of the waveform is clearly evident; a change in the coda of a wave in a braced medium should be expected.

More tellingly, in Figure 8, a snapshot of the wave after propagation through a braced medium is transformed to the frequency (i.e., k_x) domain and the classical and KG spectra

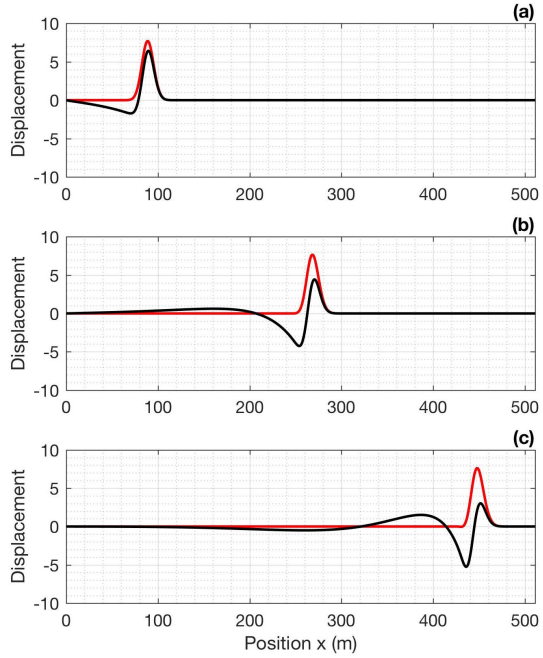

FIG. 7. 1D snapshots of pulses obeying (red) the classical wave equation versus (black) the KG equation. (a)-(c) Three times, early, mid, and late in the propagation. The dispersion and coda features of a KG field are evident.

are compared. The leading order features of the KG field is the strong suppression of the low frequency components and the mild increase of the high frequency components (Figure 8b).

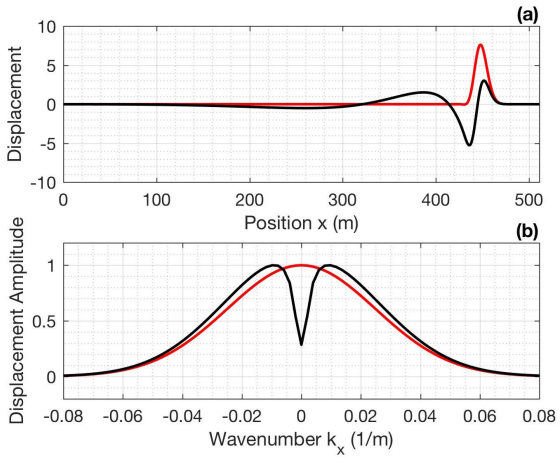

FIG. 8. Comparisons of (a) time-domain pulses and (b) wavenumber domain spectra of classical wave solutions (red) versus KG solutions (black). Apparent in (b) is the leading order feature of KG fields versus classical waves, which is the suppression of low frequencies, occurring in homogeneous braced media.

Hypothesis

The hypothesis we will now analyze and attempt to support is as follows. The presence of the microbubble fluid within the silt injection zone (when analyzed with kHz range

seismic waves), and the CO_2 as it enters the formation (when analyzed with 10-100Hz range seismic waves), are both causing the medium supporting the seismic waves to *act as if additional resistance to the seismic motion in the form of bracing is present.*

SEISMIC WAVES IN A BRACED ISOTROPIC-ELASTIC MEDIUM

To make more practical use of the features of a KG field, that is, to assume that the fluid/gas flowing into the formation rocks is causing seismic waves to behave as if they were experiencing elastic bracing, we must next extend beyond a 1D scalar-acoustic setting, and allow elastic displacements to occur within multidimensional solid media. To this end we adapt a displacement-stress finite difference code written by CREWES PDF J. Li for isotropic-elastic wave propagation as follows. The code, its basic formulation and PML framework, derives from the anisotropic framework of Li et al. (2017) in the isotropic limit. The equations derive from the elastodynamic force balance holding in a source-free volume of space:

$$\rho \ddot{u}_i - \sigma_{ij,j} = 0, \tag{4}$$

where σ_{ij} and u_i represent the stress tensor and displacement vector respectively. To incorporate elastic bracing, we hypothesize a second restoring force (to complement Hooke's law as used in the stress calculations), which is proportional to displacement u_i:

$$\rho \ddot{u}_i - \sigma_{ij,j} - \eta u_i = 0. \tag{5}$$

The quantity η is a property of the medium, akin to velocity, density, Q, etc., which controls the degree of bracing resistance; as $\eta \to 0$, equation (5) and all phenomena simulated based on it lapse to those associated with standard linear elasticity. This alteration of the equation of motion transfers straightforwardly into the finite difference code. In original form each component of displacement (e.g., $\{u, v, w\}$) is updated according to

$$u_{i,j}^{n+1} = 2u_{i,j}^{n} - u_{i,j}^{n-1} + \frac{\Delta t^2}{\rho_{i,j}} \times \text{stress terms}, \tag{6}$$

where i and j are indices representing lateral position and depth respectively, and $n-1$, n and $n+1$ are the previous, current and future time indices. To incorporate elastic bracing, the factor 2 in equation (6) is simply reduced by the amount η, which we permit to be spatially varying:

$$u_{i,j}^{n+1} = \big(2 - \eta_{i,j}\big) u_{i,j}^{n} - u_{i,j}^{n-1} + \frac{\Delta t^2}{\rho_{i,j}} \times \text{stress terms}. \tag{7}$$

Numerical simulations

To simulate numerically the effect of elastic bracing, a model with similar features as the JOGMEC experiment is synthesized. For numerical convenience, the model is scaled up spatially by roughly $10\times$, and illuminated by seismic waves on a frequency range scaled down by roughly $10\times$. The model is illustrated in Figure 9.

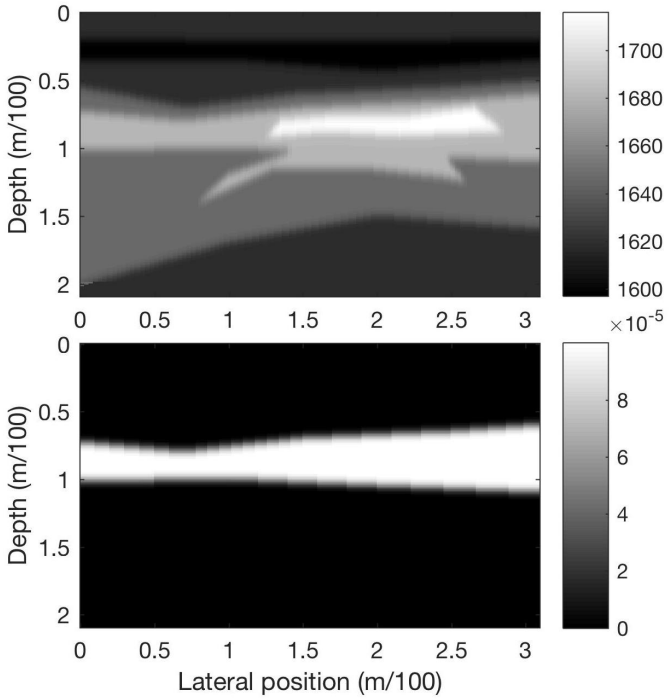

FIG. 9. Model for 2D simulation of seismic waves in an elastically-braced isotropic solid. Upper panel: P-wave velocity; lower panel: bracing parameter η. This model is designed to resemble the JOGMEC medium, but for convenience in numerical modelling has been increased in spatial scale by a fact of approximately 10 (the frequencies used are likewise scaled down by a factor of approximately 10).

With the elastic finite difference code adapted as per equation (7), and the parameters chosen as in Figure 9, a waveform is propagated across the medium to produce synthetic cross-well data. The wave is propagated twice, once with a finite η and once with $\eta = 0$, so the waveforms can be compared. In Figure 10, snapshots of the waveform as it propagates are plotted, once (top left) as it appears within the η model, again (top right) as it appears within the velocity model, and once as a single snapshot along the lateral coordinate at the depth of the source.

In Figure 10 a single trace from a receiver at the far right of the model (same depth as source) is extracted and plotted (left panel) for both the un-braced (black) and and braced (red) media. The spectra are likewise overlain on each other in the right panel. Comparing the black (baseline) and the red (braced) fields, we find that with little "effort" (in the sense of introducing specially made heterogeneities) we have reproduced all four of the features observed in the JOGMEC data: strong reduction of low frequencies, mild increase of high frequencies, coda and even a low frequency notch.

DISCUSSION

There appear to be a growing set of anecdotal reports in our community, to the effect that waveforms undergo complex changes as they pass regions where gas/fluid mixtures are being injected into reservoir zones. Full theories describing mechanical waves in such media would certainly include poroelasticity, and high levels of spatial heterogeneity.

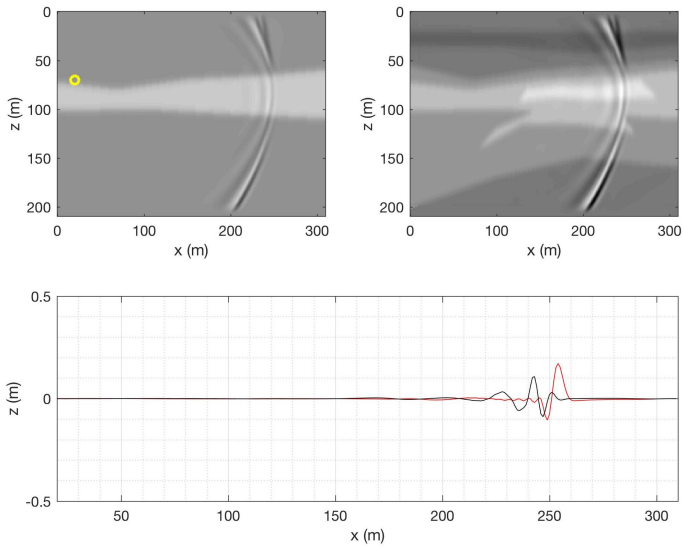

FIG. 10. Snapshots of the wave propagating through the 2D solid elastically-braced medium. Top left: η model; top right: velocity model; bottom: snapshot of the waveform along the x coordinate with z fixed at the depth of the source (red: elastic wave with $\eta = 0$; black: braced waveform with $\eta \neq 0$.

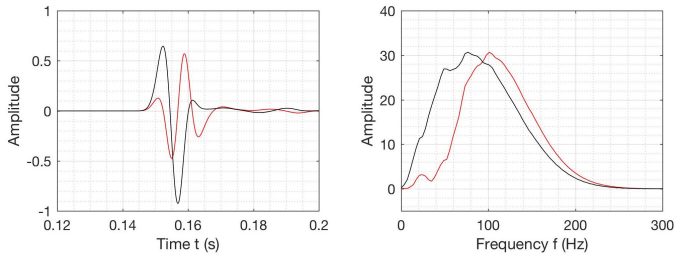

FIG. 11. Extracted crosswell traces for the un-braced (black) and braced (red) media. Left panel: time domain; right panel: frequency domain. Compare with Figures 3a-b.

However, the utility of introducing a very large and complex set of parameters in order to reproduce and characterize these phenomena would have to be questioned. Certainly, seismic measurements cannot be expected to constrain a large number of extra parameters, and often the heterogeneities needed to reproduce complex phenomena themselves must occur well below the resolving power of a seismic experiment.

In the past it has generally been only when macroscopic consequences of microscopic phenomena have (a) bled through to seismic scales, and (b) availed themselves of accurate macroscopic modelling, that the phenomena have permitted stable parameter inversion and interpretation. The classical examples of this are viscoelasticity, and its introduction of a few macroscopic parameters, e.g., Q_P and Q_S, and anisotropy (with its γ, δ, ϵ). The best possible outcome of this initial investigation would be to find that inverted maps of the parameter η were stably derivable and delineated and quantified useful injected fluid properties. Whether or not such a think is possible is not known, and remains a tantalizing possibility only.

We have not derived from first principles a KG equation - rather we have guessed that it holds based on its circumstantial reproduction of all of the macroscopic features seen in

a field data case. Our only "proof" that elastic bracing is in effect is the ease with which we describe these features; more examples are needed before the case is fully convincing.

Still, what is compelling about the possibility that complex microscopic and/or mesoscopic dynamical effects are appearing on seismic scales in the form of effective elastic bracing, is that it allows us to consider stably determining a bracing parameter (or maps of a bracing parameter), and thereafter attempting to interpret these in terms of some microscopic model. A new mode of seismic investigation of fluid storage, injectivity, chemical/physical state, etc., would not go amiss.

CONCLUSIONS

A circumstantial case is made that the complex dynamical response of a medium containing microscopic (or at any rate, far subresolution) gas-fluid mixtures, in comparison with that measured prior to its injection, has a relatively simple macroscopic expression, is made. The macroscopic effect on the wave is that it acts as if it was experiencing elastic bracing, an additional resistance to distortion that is proportional to displacement. Homogeneous elastically-braced media reproduce field effects of lost low frequencies, boosted high frequencies, and coda and notch effects, as is shown with several synthetics. The CaMI-FRS is an ideal site to continue seeking evidence for or against our hypothesis; as would bes further microbubble scale experiments.

ACKNOWLEDGEMENTS

We thank the sponsors of CREWES for continued support. This work was funded by CREWES industrial sponsors, NSERC (Natural Science and Engineering Research Council of Canada) through the grant CRDPJ 461179-13, and in part thanks to the Canada First Research Excellence Fund. JOGMEC and especially researchers A. Kato, T. Mouri and I. Kurosawa are gratefully acknowledged for permission to use the waveform data figures, in particular Figure 3 which has not yet been published; R. Kamei is thanked for permission to use figures from her Paris EAGE abstract. The elastic forward modelling in this paper was based on a modification of the finite difference code of J. Li.

REFERENCES

Innanen, K. A., Lawton, D. C., Hall, K. W., Bertram, K., and Bertram, M., 2018, Design and deployment of a prototype multicomponent das sensor: CREWES Research Reports, **30**.

Kamei, R., Jang, U. G., Lumley, D., Mouri, T., Nakatsukasa, M., Kato, A., and Takanashi, M., 2017, Time-lapse full waveform inversion for monitoring near-surface microbubble injection, *in* Proceedings of the 79th EAGE conference & exhibition, Paris, FRA, EAGE.

Lawton, D. C., Bertram, M., Hall, K. H., and Bertram, K., 2015, New approaches to seismic monitoring at the brooks field research station: CREWES Research Reports, **27**.

Lawton, D. C., Isaac, H., and Bertram, M., 2018, Shear wave land streamer: CREWES Research Reports, **30**.

Li, J., Innanen, K. A., Tao, G., Zhang, K., and Lines, L. R., 2017, Wave field simulation of 3D borehole dipole radiation: Geophysics, **82**, No. 3, D155–D169.

Morse, P. M., and Feshbach, H., 1953, Methods of theoretical physics: McGraw-Hill Book Co.

Spackman, T., and Lawton, D. C., 2018, Processing and analysis of borehole permanent source data: CREWES Research Reports, **30**.